ACS APPLIED MATERIALS & INTERFACES

Research Article

www.acsami.org

Organic Functionalization of 3C-SiC Surfaces

Sebastian J. Schoell,[†] Matthias Sachsenhauser,[†] Alexandra Oliveros,[‡,¶] John Howgate,[†] Martin Stutzmann,[†] Martin S. Brandt,[†] Christopher L. Frewin,[‡] Stephen E. Saddow,[‡,¶] and Ian D. Sharp*[,†,§]

[†]Walter Schottky Institut and Physik-Department, Technische Universität München, Am Coulombwall 4, 85748 Garching, Germany

[‡]Electrical Engineering Department, University of South Florida, Tampa, Florida, United States

[¶]Department of Molecular Pharmacology and Physiology, University of South Florida, Tampa, Florida, United States

ABSTRACT: We demonstrate the functionalization of *n*-type (100) and (111) 3C-SiC surfaces with organosilanes. Self-assembled monolayers (SAMs) of amino-propyldiethoxymethylsilane (APDEMS) and octadecyltrimethoxysilane (ODTMS) are formed via wet chemical processing techniques. Their structural, chemical, and electrical properties are investigated using static water contact angle measurements, atomic force microscopy, and X-ray photoelectron spectroscopy, revealing that the organic layers are smooth and densely packed. Furthermore, combined contact potential difference and surface photovoltage measurements demonstrate that the heterostructure functionality and surface potential can be tuned by utilizing different organosilane precursor molecules. Molecular dipoles are observed to significantly affect the work functions of the modified surfaces. Furthermore, the magnitude of the surface band bending is reduced following reaction of the hydroxylated surfaces with organosilanes, indicating that partial passivation of electrically active surface states is achieved. Micropatterning of organic layers is demonstrated by lithographically defined oxidation of organosilane-derived monolayers in an oxygen plasma, followed by visualization of resulting changes of the local wettability, as well as fluorescence microscopy following immobilization of fluorescently labeled BSA protein.

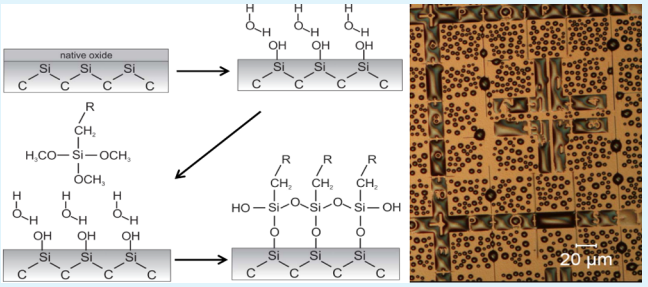

KEYWORDS: *silicon carbide, monolayer, functionalization, surface photovoltage, work function, XPS*

INTRODUCTION

Organic functionalization of semiconductor surfaces is attracting increasing interest for applications in the fields of biotechnology, biosensing, and bioelectronics. Due to its technological maturity, silicon is most commonly used as a substrate material for such applications. However, its poor chemical stability limits its use for long-term in vivo applications.[1] Additionally, ion diffusion in silicon oxide can lead to electronic drifts and high levels of electronic noise. Due to these limitations, alternate material systems are actively investigated for operation in potentially harsh biological environments. For example, diamond offers superior biocompatibility as well as chemical and mechanical stability as a substrate material. Furthermore, hydrogen termination of diamond, which can be achieved by hydrogen microwave plasma treatment, leads to the formation of surface conductive layers which are suitable for applications such as low-noise solution gated field-effect transistors for bioelectronic applications.[2,3] Although diamond is a promising material for biomedical applications, the absence of a shallow *n*-type donor, the relatively poor quality of thin film material, and expensive production costs have, to date, limited its practical use.

Silicon carbide (SiC) is a compound group-IV semiconductor composed of a 1:1 stoichiometric ratio of silicon and carbon, which exhibits many of the advantages of its elemental components. For example, this material offers a high degree of chemical, as well as mechanical, stability and is highly compatible with processing technologies evolved from silicon device fabrication.[4] Furthermore, it has been demonstrated that SiC is biocompatible and, thus, it is widely considered to be extremely promising for biomedical and biosensing applications. Among the more than 200 different crystal structures of SiC, the most commonly used polytypes are 4H- and 6H-SiC, which exhibit hexagonal crystal structure and can be grown in bulk form. In addition, the cubic phase, 3C-SiC, can be grown by chemical vapor deposition (CVD) on silicon substrates and has therefore attracted great interest for electronics, microelectromechanical systems (MEMS), and bio-MEMS applications.[5−12]

An important requirement for stable heterostructures between biomolecules and semiconductors is the formation of functional organic layers covalently attached to the substrate surface. Such surface-bound organic layers directly influence the surface and interfacial energetics, which are particularly interesting for future biotechnological applications.[12] There exist various routes to achieve inorganic/organic heterointerfaces, including silanization, alkylation, alkoxylation, and

Received: November 20, 2012
Accepted: January 28, 2013
Published: January 28, 2013

   dx.doi.org/10.1021/am302786n | *ACS Appl. Mater. Interfaces* 2013, 5, 1393−1399

surface-initiated photopolymerization, which allow the substrate properties, including biocompatibility, to be tuned at the molecular level.[11,13−17] In particular, reaction of activated SiC surfaces with silanol and olefin anchoring groups has been demonstrated for organic functionalization of this material.[15,16,18] Recently, Nebel and co-workers reported successful electrochemical functionalization of 3C-SiC surfaces with aryldiazonium salts and further demonstrated that 3C-SiC is a promising substrate material for biosensing applications.[19] While each of these methods has been applied for functionalization of SiC surfaces, determination of the impact of organic modification on the electronic properties of SiC has not yet been investigated.

Self-assembled covalent immobilization of organosilane molecules such as octadecyltrichlorosilane (ODS) on glass substrates was first reported by Sagiv et al. in 1980.[20,21] A basic requirement for successful silanization is surface activation by termination with OH-groups that can react with alkoxy groups of organosilane molecules. However, no methods for the direct hydroxyl termination of Si surfaces are available, and organosilane functionalization of this material requires a thin oxide interlayer. In contrast, Starke and co-workers have demonstrated that etching of SiC in hydrofluoric acid leads to the formation of a hydroxyl termination.[22] Therefore, this material is ideally suited for direct wet chemical silanization without the necessity for an oxide interlayer.[18,22−25] Previously, we utilized thermal desorption measurements to confirm covalent attachment of organosilane molecules to hydroxylated 6H-SiC surfaces.[18] Here, we investigate the structural and electronic properties of organic self-assembled monolayers (SAMs) formed from amino-propyldiethoxymethylsilane (APDEMS) and octadecyltrimethoxysilane (ODTMS) on (100) and (111) 3C-SiC via wet-chemical silanization techniques.[26,27] We show that the resulting organic layers are of high quality and can be used to tune the interfacial energetics of 3C-SiC surfaces. In particular, this process allows for direct tuning of the substrate work function, which will enable additional control over the energetic alignment of the band edges with respect to redox levels in solution. Furthermore, the reduction of the surface band bending following reaction with organosilane molecules indicates partial passivation of surface states and is expected to reduce surface recombination. These results indicate that such systems are promising for applications in bio- and molecular electronics.

EXPERIMENTAL SECTION

Materials. The 3C-SiC layers used in this work were grown in a horizontal, low pressure, CVD reactor on (100) and (111) silicon substrates at 1375 °C, followed by moderate etching in Pd-purified hydrogen in order to reduce the surface defect concentration.[8,28,29] Organic solvents and amino-propyldiethoxymethylsilane (97%) were purchased from Sigma-Aldrich (Munich, Germany), and octadecyltrimethoxysilane (95%) was purchased from ABCR GmbH (Karlsruhe, Germany). All chemicals were used without additional purification.

Silanization Reaction. Figure 1 shows a schematic illustration of the functionalization process. Prior to reaction, all samples were ultrasonically cleaned in acetone and isopropanol for 10 min each, followed by two cycles of oxygen plasma cleaning (300W, 1.4 mbar) and etching in 5% hydrofluoric acid (HF) in H_2O for 5 min. Surface hydroxylation was achieved by a final 5 min HF treatment immediately prior to the functionalization reaction. APDMES functionalization was performed at room temperature in a glovebox under Ar atmosphere (O_2 < 1 ppm, H_2O < 2 ppm) in order to prevent oligomerization of the molecules during the process. For functionalization with ODTMS, 0.5% butylamine was added to the reaction solution as a catalyst. In

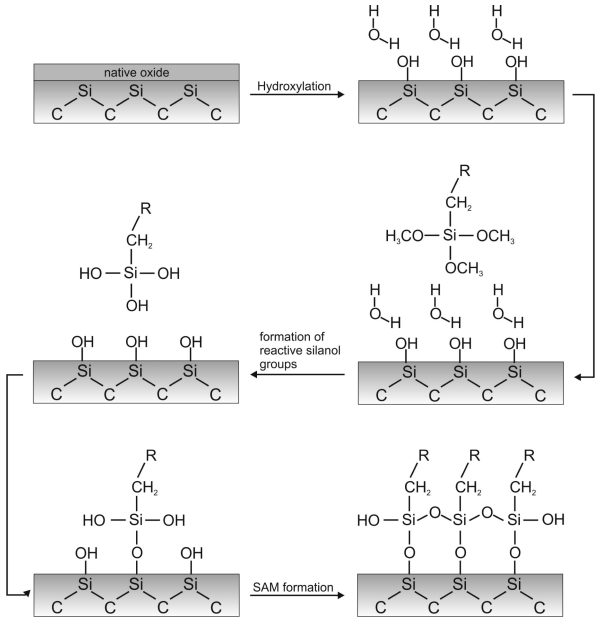

Figure 1. Schematic illustration of the wet chemical organosilanization process. In the first step, the native oxide was removed by treatment in hydrofluoric acid, resulting in hydroxylation of surface sites. Self-assembly was achieved by immersing hydroxylated samples in a solution containing the desired organosilane molecules. This illustration is representative of the expected interfacial bonding configuration following reaction with ODTMS, which possesses three methoxy headgroups. However, the bifunctional anchoring group of APDEMS is expected to reduce the degree of interfacial Si−O−Si bonding.

both cases, the samples were immersed in 5% solutions of organosilane molecules in toluene at 14 °C for 90 min. We note that both temperature and relative humidity significantly affect monolayer quality, as demonstrated by Desbief et al.,[30] as well as references therein. Following ODTMS silanization, the samples were ultrasonically cleaned twice in toluene and methanol for 30 min each, in order to remove any physisorbed molecules from the surface. For the case of APDEMS functionalization, the cleaning process consisted of ultrasonic treatment in toluene and isopropanol for 30 min each.

To provide the correct chemical functionality for binding proteins, a Schiff-base formation was carried out by immersing patterned APDEMS functionalized samples in a solution of glutaric dialdehyde in deionized-water for 1 h at room temperature. This cross-linker binds to the remaining functional amine groups and enables local attachment of Alexa488 labeled BSA proteins. Fluorescence microscopy measurements were performed using a Zeiss Axiovert 200 M Mat microscope.

Static Water Contact Angle Measurements. All data were acquired using a custom built static water contact angle measurement setup. Droplets of 3 μL of deionized water (ρ = 18 MΩ·cm) were deposited onto the surfaces of the samples, and images were acquired using a video camera. Contact angle evaluation was carried out using standard image processing software. All contact angle values are given with an accuracy of ±1°.

Atomic Force Microscopy. Atomic force microscopy (AFM) images were acquired with a Digital Instruments MultiMode system in tapping-mode using silicon tips at scan frequencies between 0.5 and 0.8 Hz. Image processing, including analysis of step heights, surface roughness, and homogeneity were performed using Nanoscope software as well as the free software suite WSxM from Nanotec Electronica S.L. (Spain).[31]

X-ray Photoelectron Spectroscopy. Measurements were performed in an ultrahigh vacuum system equipped with a SPECS XR-50 Mg-Anode X-ray source (E_{K_α} = 1253.6 eV). Photoelectrons

were detected using a SPECS Phoibos 100 hemispherical analyzer with an MCD-5 detector. Unless otherwise noted, all data presented in this work were acquired using a pass energy of 25 eV at a takeoff angle of 0° relative to the surface normal. The examined area was adjusted to ≈7 mm^2 using a combination of a mechanical aperture, entrance and exit slits, and electron optics of the analyzer. For analysis, the raw data were processed by subtraction of linear or Shirley backgrounds and fitted with quasi-Voigt functions using the software CasaXPS provided by SPECS GmbH (Berlin, Germany).

Contact Potential Difference and Surface Photovoltage Measurements. Contact potential difference (CPD) and surface photovoltage (SPV) measurements allow for nondestructive and contact-less investigation of the surface energetics of semiconductors and metals. Measurements of the CPD in darkness, along with light-induced changes of the surface voltage, allow for quantitative investigation of surface and interface properties, such as surface band bending, surface charge, and interfacial dipoles. In particular, exposure of the sample to sufficiently intense above-band gap light leads to the formation of split quasi-Fermi levels, screening of surface charges, and a corresponding flattening of the surface band bending. Hence, changes in the CPD value under illumination give a direct measure for the surface band bending. All CPD and SPV data presented in this work were acquired under ultrahigh vacuum using a Besocke Delta Phi Kelvin Probe S vibrating gold mesh electrode controlled by a Besocke Kelvin Control 07 unit from Besocke Delta Phi GmbH (Jülich, Germany). Illumination was provided by a low pressure Hg lamp (Benda, Germany), and signal saturation measurements were performed to ensure accurate determination of the surface photovoltage.

RESULTS AND DISCUSSION

After the initial cleaning and HF etching procedures, both (100) and (111) 3C-SiC surfaces exhibited hydrophilic behavior consistent with the reported hydroxyl termination following HF treatment of SiC,[22] with static water contact angles of <5°. ODTMS-modified samples were characterized by contact angles of up to 92° on the (100) surface and 96° on the (111) surface, indicating formation of hydrophobic layers due to terminal CH_3-groups (Table 1). It is expected that further optimization of this procedure could yield higher contact angles, such as those demonstrated by Rosso and co-workers following thermal and UV activated olefin reactions on SiC.[15,16] Following functionalization with APDEMS, contact angles of 55° and 58° were observed on the (100) and (111) surfaces, respectively, which are characteristic of the terminal amine end groups.[26] Figure 2 shows atomic force micrographs of hydroxylated and subsequently organosilane-modified surfaces. Roughness analysis and comparison of the morphologies of modified and hydroxylated surfaces are consistent with the formation of organic overlayers without reactant oligomerization during the functionalization process (Table 1). The observed morphological differences between (100) and (111) surfaces are characteristic of the growth process and hydrogen treatment.

Table 1. Summary of Wetting Behavior Investigated by Static Water Contact Angle Measurements (CA) and Surface Roughnesses Obtained by AFM Analysis[a]

	(100) 3C-SiC		(111) 3C-SiC	
treatment	rms (nm)	CA (deg)	rms (nm)	CA (deg)
HF	1.6	<5	3.3	<5
APDEMS	1.7	55	3.3	58
ODTMS	1.6	92	3.2	96

[a]For the case of (100) surfaces, rms values were obtained from plateaus in order to exclude the large morphological features that are characteristic of the growth process.

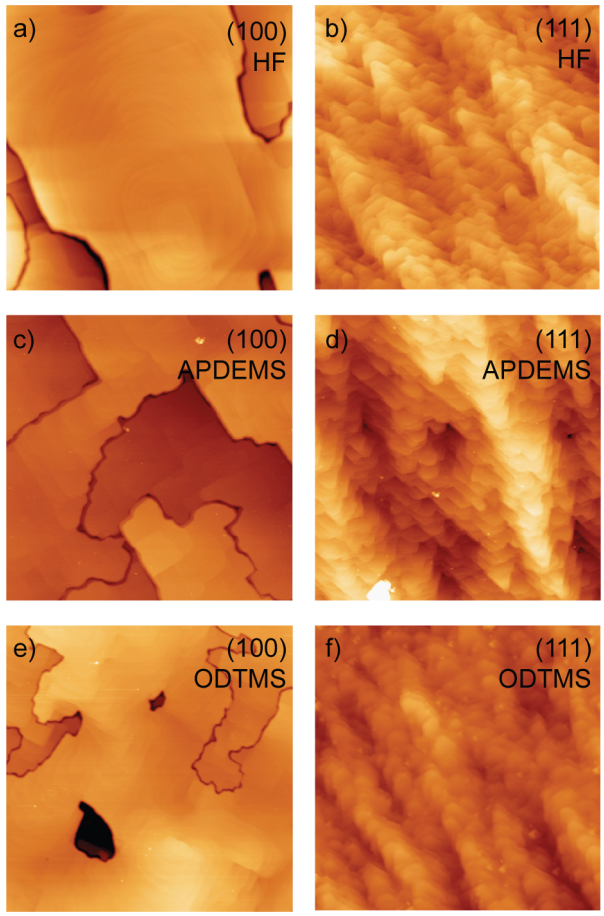

Figure 2. AFM micrographs (5 × 5 μm^2, z scale 50 nm) of hydroxylated (a) (100) and (b) (111) 3C-SiC. (c) and (d) show corresponding APDEMS-modified surfaces, and (e) and (f) show corresponding ODTMS-modified surfaces.

In order to determine the chemical composition of the surfaces, X-ray photoelectron spectroscopy (XPS) was performed. Although SiC is attracting increasing interest for technological applications, relatively few studies have been carried out on hydroxylated 3C-SiC.[32] Since the chemical composition of the semiconductor surface is of great importance for the realization of monolayers, we first focus on the hydroxylation of 3C-SiC surfaces via wet-chemical etching in hydrofluoric acid. Figure 3 shows XPS survey and core level spectra of (100) and (111) 3C-SiC surfaces following the standard cleaning and HF treatment procedure. The survey scans from both surfaces reveal peaks at 101.2, 151.0, and 283.4 eV, which can be attributed to the Si2p, Si2s, and C1s substrate core levels, respectively. In addition, a strong O 1s signal is observed at 534 eV, which is consistent with the expected hydroxyl surface termination of HF-treated SiC. High resolution scan data reveal that the Si2p core level spectra can be deconvoluted into doublets with a 0.6 eV splitting and a branching ratio of 1:2, due to spin−orbit splitting. Although no pronounced oxidic component can be resolved, an additional weak component is observed at 103 eV, which is indicative of silicon in the Si^{2+} oxidation state. In addition, deconvolution of the C1s core level spectra yields an additional component at ≈285 eV, which can be attributed to hydrocarbons at the

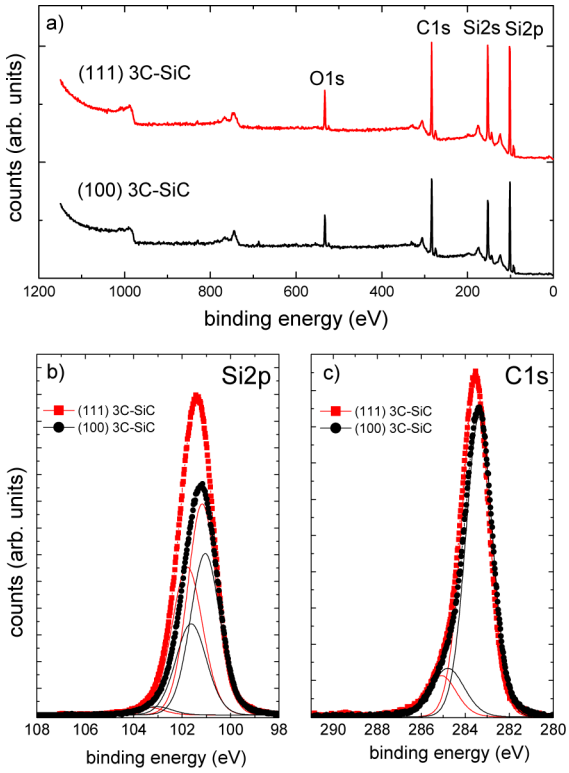

Figure 3. (a) XPS survey spectra of HF-etched (100) (black) and (111) (red) 3C-SiC. (b) Si2p and (c) C1s core level spectra. The solid lines in (b) and (c) give the fitted spectral components of the deconvoluted data.

surface (Figure 3c). Together, these findings are similar to previously published studies on hexagonal SiC crystals, which revealed that etching in HF leads to the formation of predominantly hydroxylated surfaces.[33] The possibility of wet-chemical surface hydroxylation renders 3C-SiC a promising candidate for functionalization with organosilane molecules according to the well-established silanization routes.

Using the functionalization methods described in the Experimental Section, hydroxylated samples were modified with either APDEMS or ODTMS molecules. Figure 4a shows XPS survey scans of APDEMS-modified (111) and (100) 3C-SiC surfaces. Following surface modification with organosilanes, attenuation of the substrate peaks occurs due to the overlying organic layers. A layer thickness of 10 Å was derived from the attenuation of the substrate-related C1s core level signal, which is in good agreement with the theoretical value for a monolayer of 8.5 Å. However, we note that the layer thickness calculation was performed on the basis of electron attenuation lengths obtained from reference data on alkanethiol monolayers on Au and the resulting value should be taken as an estimate only.[34] In addition to the substrate-related signal at 283.4 eV, an additional component appears at 285.5 eV (Figure 4b), which is characteristic of hydrocarbons on the surface and was also observed in previous reports on organosilane modified 6H-SiC and silicon.[18,35] As shown in Figure 4c,d, surface modification with APDEMS results in two N1s core level spectral components, which can be resolved at 400 and 402.5 eV and arise from terminal NH_2 and NH_3^+ groups, respectively.[36−38] We observe a ratio of 2:1 for the NH_2/NH_3^+ intensity, which is similar to the findings reported by Bierbaum et al. for organosilane-modified oxidized silicon surfaces.[36] This result

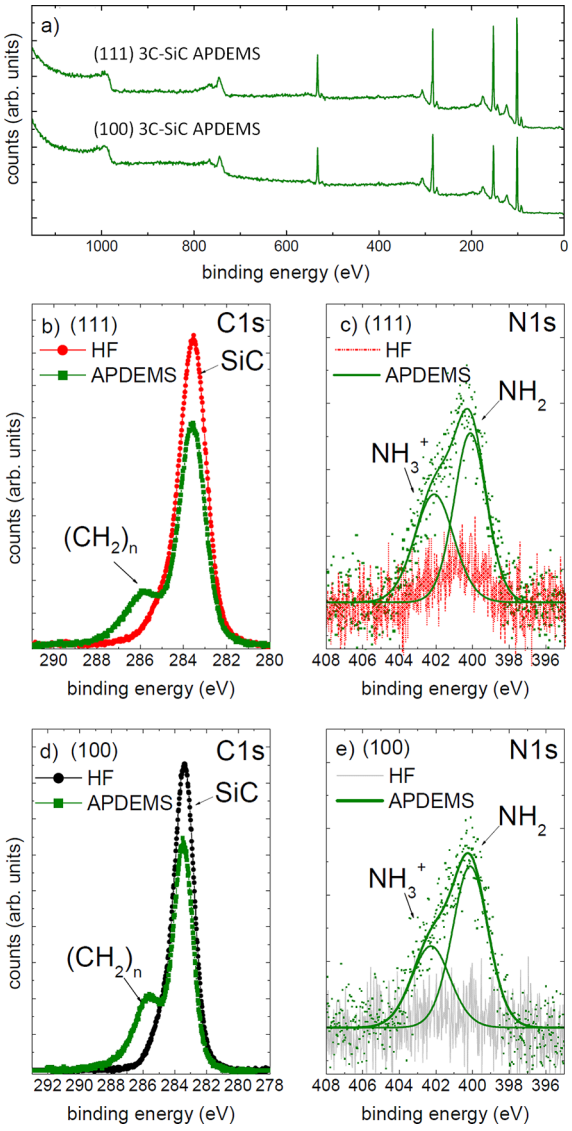

Figure 4. (a) XPS survey spectra of APDEMS-modified (111) and (100) 3C-SiC. (b) C1s and (c) N1s core level spectra for (111) 3C-SiC. (d) and (e) show corresponding C1s and N1s core level spectra for (100) 3C-SiC. Fitted spectral components in (c) and (e) are given by the solid lines.

demonstrates the effective formation of thin organic layers with a high concentration of reactive NH_2 groups present at the surface, which could allow for attachment of more complex biomolecules such as proteins and DNA. Similar results are obtained for (100) 3C-SiC surfaces following functionalization with APDEMS, as demonstrated in Figure 4d,e. Although the present XPS analysis does not provide direct spectroscopic evidence of covalent bonding between the molecules and substrate, these results are consistent with previous results that indicated covalent attachment of organosilane molecules on 6H-SiC, which also exhibits a hydroxyl-terminated surface following HF etching.[18]

Attachment of organic layers can lead to changes of the surface dipole layer, which directly affect the work function, Φ_s, of the material. The work function is defined as the difference between the Fermi level, E_F, and vacuum level, E_{vac}. Formation of surface dipoles upon attachment of adlayers leads to steps in the local vacuum level of magnitude $\Delta\Phi_s$. In order to

dx.doi.org/10.1021/am302786n | ACS Appl. Mater. Interfaces 2013, 5, 1393−1399

determine the effect of SAM formation on the energetics of 3C-SiC surfaces, contact potential difference (CPD) measurements were performed using a gold mesh reference electrode under vacuum conditions. The ability to tune the semiconductor work function provides a means of engineering the electronic alignment of the semiconductor valence and conduction bands with external systems, such as metals, molecules, or electrochemical redox species, which is important for applications ranging from solid state and molecular electronics to biosensing.

Following HF etching, (100) and (111) 3C-SiC exhibited dark CPD values of +0.5 and +0.4 eV, respectively. These values correspond to large work functions which are associated with the formation of negative surface dipoles due to the surface termination with hydroxyl groups. For ODTMS-modified surfaces, the CPD values decrease to +0.2 eV on both crystal orientations, indicating that the reaction of oxygen-terminated surfaces to form methyl-terminal SAMS and an Si−O−Si cross-linked interlayer (see Figure 1) reduces the work function of the material. After functionalization with APDEMS, the CPD values decreased to −0.5 eV for both surfaces. The large change of 0.9 eV compared to the HF-treated surfaces is in agreement with XPS results and indicates a transition from the oxygen-induced negative surface dipole to a positive dipole associated with the terminal NH_2 and NH_3^+ groups. In order to gain more knowledge about the influence of organic modification on the electrical properties at the bio/inorganic interface, surface photovoltage measurements were performed. The surface band bending for hydroxylated surfaces was observed to be ≈220 mV. This suggests a high concentration of electrically active defect sites on both (100) and (111) surfaces and is consistent with previous studies on hydroxylated 6H-SiC, which exhibits even larger SPV values of ≈400 mV.[22,23,39,40] Following organic modification with either ODTMS or APDEMS, both (100) and (111) surfaces exhibit reduced surface band bending with SPV values between 120 and 180 mV, indicative of a successful reduction of surface defect sites by the attachment of the organic overlayer. The reduced band bending at the bio/inorganic interface is of great importance for bioelectronic applications allowing for reduced surface recombination and improved charge transfer accross the interface. These results are summarized in the schematic illustration of the surface energetics of hydroxylated and APDEMS-modified surfaces in Figure 5, as well as the summary of CPD and SPV data presented in Figure 6.

Spatial control over protein adsorption properties by, for example, locally controlling the surface hydrophobicity, is known to enable the permissiveness of the surface for cells to be tuned.[41−44] Previously, Rosso and co-workers demonstrated a process based on short (0.5−3 s) oxygen plasma treatments

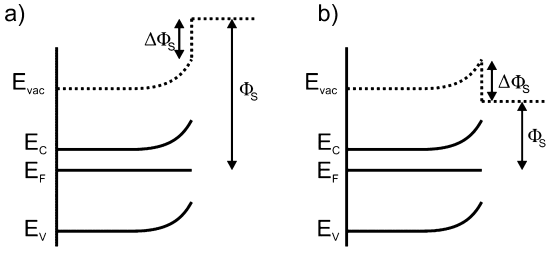

Figure 5. Schematic band diagrams for 3C-SiC surfaces after (a) OH-termination by HF etching and (b) functionalization with APDEMS.

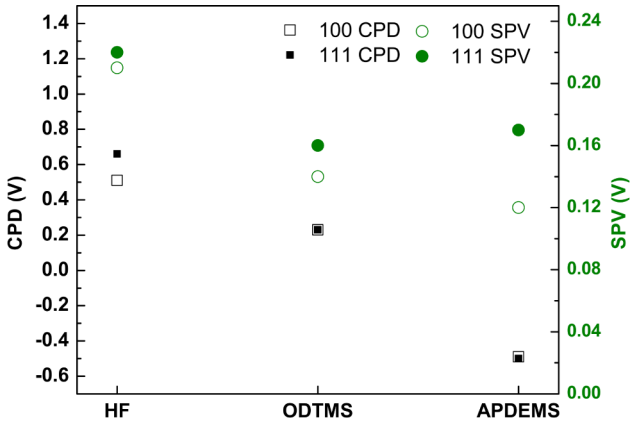

Figure 6. Summary of CPD and SPV data following different surface treatments.

to introduce functional moieties on initially methyl-terminal SAMs on silicon and silicon nitride surfaces.[45] Here, we adapt this technique to provide surfaces with spatially controlled wetting behavior via 5 min oxygen plasma treatments. After functionalization with ODTMS, the SAM was patterned by conventional photolithography. Subsequent oxygen plasma treatment resulted in local destruction of the hydrophobic organic layer and formation of hydrophilic oxidized regions on the surface. Figure 7a shows XPS survey scans of ODTMS-modified (green), as well as oxygen-plasma exposed (black), surfaces. Following plasma treatment, a pronounced increase of the peak in the O1s core level region at 534 eV is observed,

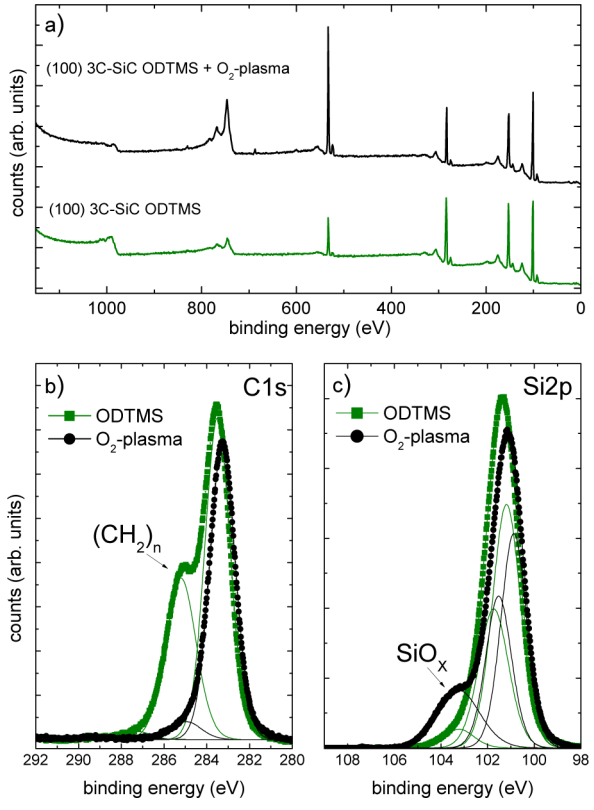

Figure 7. (a) XPS survey spectra of ODTMS-modified (green) and subsequently O_2-plasma treated (black) (100) 3C-SiC. (b) C1s and (c) Si2p core level spectra reveal degradation of the organic overlayer and oxide growth upon exposure to O_2-plasma.

dx.doi.org/10.1021/am302786n | ACS Appl. Mater. Interfaces 2013, 5, 1393−1399

which arises from surface oxidation. Furthermore, an additional component at 103.5 eV in the Si2p core level spectrum (Figure 7c) arises, which confirms formation of a silicon suboxide at the surface. Inspection of the C1s core level spectrum reveals that the plasma treatment leads to a complete removal of the peak at 285.5 eV (Figure 7b).

Figure 8a shows an optical micrograph highlighting the wettability contrast of a micropatterned ODTMS-modified 3C-SiC surface. The change of wettability was visualized by exposure of the surface to water vapor, which led to preferential condensation on the more hydrophilic plasma-exposed regions. This result confirms that ODTMS SAMs survive the lithography process and that local modification of surface properties is possible using standard semiconductor processing methods. In a separate experiment, the plasma-based micropatterning procedure was applied to an APDEMS-modified surface. Fluorescently labeled BSA proteins were then immobilized on the patterned surface using glutaric dialdehyde linkers. Fluorescence optical microscopy indicates that immobilization is successful and occurs selectively in non-plasma exposed regions, as shown in Figure 8b. Therefore, it is possible to conclude that the terminal amine groups of the APDEMS-derived monolayer are chemically reactive following the patterning procedure.

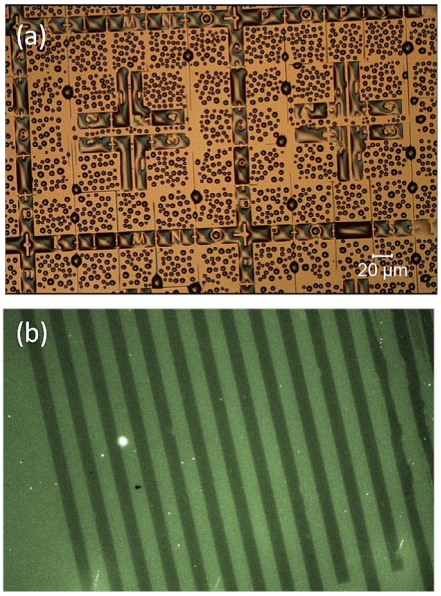

Figure 8. (a)Wettability contrast image of a micropatterned ODTMS-modified 3C-SiC surface by optical microscopy. Water droplets condense preferentially in hydrophilic oxygen plasma-exposed regions. (b) Fluorescence optical micrograph (50× magnification) of a 3C-SiC surface following micropatterning of the ODTMS layer and immobilization of fluorescently labeled BSA protein.

CONCLUSION

We have demonstrated chemical functionalization of both (100) and (111) 3C-SiC with organosilane molecules. Spatially controlled hydrophobicity and protein immobilization was shown by micropatterning of ODTMS monolayers, thereby demonstrating the possibility of locally modifying the surface properties. Additionally, we have shown that the work function of 3C-SiC can be tuned by altering the surface dipole layer using organosilane molecules and that reaction results in a partial passivation of undesirable surface states. In combination, these methods can be utilized for engineering SiC surface biocompatibility for bioelectronic applications, such as spatially controlled cell adhesion in lab-on-a-chip environments. Furthermore, functionalization with amine-terminal APDEMS molecules will allow for the attachment of more complex biomolecules, thus rendering 3C-SiC a promising material for future biotechnological applications.

AUTHOR INFORMATION

Corresponding Author

*E-mail: idsharp@lbl.gov.

Present Address

[§]Joint Center for Artificial Photosynthesis, Lawrence Berkeley National Laboratory, 1 Cyclotron Rd., Berkeley, CA 94720.

Notes

The authors declare no competing financial interest.

ACKNOWLEDGMENTS

S.J.S. acknowledges support by the IGSSE and CompInt graduate schools at TU München. I.D.S. and S.J.S. acknowledge financial support of the Technische Universität München - Institute for Advanced Study, funded by the German Excellence Initiative.

REFERENCES

(1) Rousche, P.; Normann, R. *J. Neurosci. Methods* **1998**, *82*, 1−15.
(2) Hauf, M.; Hess, L.; Howgate, J.; Dankerl, M.; Stutzmann, M.; Garrido, J. *Appl. Phys. Lett.* **2010**, *97*, 093504.
(3) Dankerl, M.; Lippert, A.; Birner, S.; Stützel, E. U.; Stutzmann, M.; Garrido, J. A. *Phys. Rev. Lett.* **2011**, *106*, 196103.
(4) Saddow, S.; Agrawal, A. *Advances in Silicon Carbide Processing and Applications*; Norwood: Artech House, MA, 2004.
(5) Fisher, G.; Barnes, P. *Philos. Mag. B* **1990**, *61*, 217−236.
(6) Botsoa, J.; Lysenko, V.; Geloen, A.; Marty, O.; Bluet, J. M.; Guillot, G. *Appl. Phys. Lett.* **2008**, *92*, 173902.
(7) Frewin, C. L.; Jaroszeski, M.; Weeber, E.; Muffly, K. E.; Kumar, A.; Peters, M.; Oliveros, A.; Saddow, S. E. *J. Mol. Recognit.* **2009**, *22*, 380−388.
(8) Coletti, C.; Jaroszeski, M. J.; Pallaoro, A.; Hoff, M.; Iannotta, S.; Saddow, S. E. *IEEE Eng. Med. Biol.* **2007**, 5849−5852, DOI: 10.1109/IEMBS.2007.4353678.
(9) Gonzalez, P.; Serra, J.; Liste, S.; Chiussi, S.; Leon, B.; Perez-Amor, M.; Martinez-Fernandez, J.; de Arellano-Lopez, A. R.; Varela-Feria, F. M. *Biomaterials* **2003**, *24*, 4827−4832.
(10) Kotzar, G.; Freas, M.; Abel, P.; Fleischman, A.; Roy, S.; Zorman, C.; Moran, J. M.; Melzak, J. *Biomaterials* **2002**, *23*, 2737−2750.
(11) Yakimova, R.; Petoral, R.; Yazdi, G.; Vahlberg, C.; Spetz, A. L.; Uvdal, K. *J. Phys. D: Appl. Phys.* **2007**, *40*, 6435−6442.
(12) Stutzmann, M.; Garrido, J. A.; Eickhoff, M.; Brandt, M. S. *Phys. Status Solidi A* **2006**, *203*, 3424−3437.
(13) Kapur, R.; Rudolph, A. *Exp. Cell. Res.* **1998**, *244*, 275−285.
(14) Lee, M.; Brass, D.; Morris, R.; Composto, R.; Ducheyne, P. *Biomaterials* **2005**, *26*, 1721−1730.
(15) Rosso, M.; Arafat, A.; Schroën, K.; Giesbers, M.; Roper, C. S.; Maboudian, R.; Zuilhof, H. *Langmuir* **2008**, *24*, 4007−4012.
(16) Rosso, M.; Giesbers, M.; Arafat, A.; Schroën, K.; Zuilhof, H. *Langmuir* **2009**, *25*, 2172−2180.
(17) Steenackers, M.; Sharp, I. D.; Larsson, K.; Hutter, N.; Stutzmann, M.; Jordan, R. *Chem. Mater.* **2010**, *22*, 272−278.
(18) Schoell, S. J.; Hoeb, M.; Sharp, I. D.; Steins, W.; Eickhoff, M.; Stutzmann, M.; Brandt, M. S. *Appl. Phys. Lett.* **2008**, *92*, 153301.
(19) Yang, N.; Zhuang, H.; Hoffmann, R.; Smirnov, W.; Hees, J.; Jiang, X.; Nebel, C. E. *Anal. Chem.* **2011**, *83*, 5827−5830.
(20) Sagiv, J. *J. Am. Chem. Soc.* **1980**, *102*, 92−98.

(21) Ulman, A. *An Introduction to Ultrathin Organic Films*; Academic Press, London, 1991.
(22) Starke, U.; Bram, C.; Steiner, P.-R.; Hartner, W.; Hammer, L.; Heinz, K.; Müller, K. *Appl. Surf. Sci.* **1995**, *89*, 175−185.
(23) Hollering, M.; Bernhardt, J.; Schardt, J.; Ziegler, A.; Graupner, R.; Mattern, B.; Stampfl, A. P. J.; Starke, U.; Heinz, K.; Ley, L. *Phys. Rev. B* **1998**, *58*, 4992−5000.
(24) Sieber, N.; Seyller, T.; Graupner, R.; Ley, L.; Mikalo, R.; Hoffmann, P.; Batchelor, D.; Schmeisser, D. *Appl. Surf. Sci.* **2001**, *184*, 278−283.
(25) Cicero, G.; Catellani, A. *J. Chem. Phys.* **2005**, *122*, 214716.
(26) Mooney, J.; Hunt, A.; McIntosh, J.; Liberko, C.; Walba, D.; Rogers, C. *Proc. Natl. Acad. Sci. U.S.A.* **1996**, *93*, 12287−12291.
(27) Hernando, J.; Pourrostami, T.; Garrido, J. A.; Williams, O. A.; Gruen, D. M.; Kromka, A.; Steinmüller, D.; Stutzmann, M. *Diamond Relat. Mater.* **2007**, *16*, 138−143.
(28) Reyes, M.; Waits, M.; Harvey, S.; Shishkin, Y.; Geil, B.; Wolan, J. T.; Saddow, S. E. *Mater. Sci. Forum* **2005**, *527*, 307−310.
(29) Myers, R. L.; Shishkin, Y.; Kordina, O.; Saddow, S. E. *J. Cryst. Growth* **2005**, *285*, 486−490.
(30) Desbief, S.; Patrone, L.; Goguenheim, D.; Guerin, D.; Vuillaume, D. *Phys. Chem. Chem. Phys.* **2011**, *13*, 2870−2879.
(31) Horcas, I.; Fernandez, R.; Gomez-Rodriguez, J.; Colchero, J.; Gomez-Herrero, J.; Baro, A. M. *Rev. Sci. Instrum.* **2007**, *78*, 013705.
(32) Schardt, J.; Bernhardt, J.; Starke, U.; Heinz, K. *Surf. Rev. Lett.* **1998**, *5*, 181−186.
(33) Seyller, T. *J. Phys.: Condens. Matter* **2004**, *16*, S1755−S1782.
(34) Laibnis, P.; Bain, C.; Whitesides, G. *J. Phys. Chem.* **1991**, *95*, 7017−7021.
(35) Vandenberg, E. T.; Bertilsson, L.; Liedberg, B.; Uvdal, K.; Erlandsson, R.; Elwing, H.; Lundstroem, I. *J. Colloid Interface Sci.* **1991**, *147*, 103−118.
(36) Bierbaum, K.; Kinzler, M.; Woll, C.; Grunze, M.; Hahner, G.; Heid, S.; Effenberger, F. *Langmuir* **1995**, *11*, 512−518.
(37) Bui, L. N.; Thompson, M.; McKeown, N. B.; Romaschin, A. D.; Kalman, P. G. *Analyst* **1993**, *118*, 463−474.
(38) Chong, A. S. M.; Zhao, X. S. *J. Phys. Chem. B* **2003**, *107*, 12650.
(39) Sieber, N.; Mantel, B.; Seyller, T.; Ristein, J.; Ley, L. *Diamond Relat. Mater.* **2001**, *10*, 1291−1294.
(40) Johansson, L.; Owman, F.; Martensson, P. *Phys. Rev. B* **1996**, *53*, 13793−13802.
(41) Falconnet, D.; Csucs, G.; Grandin, H.; Textor, M. *Biomaterials* **2006**, *27*, 3044−3063.
(42) Kotov, N. A.; Winter, J. O.; Clements, I. P.; Jan, E.; Timko, B. P.; Campidelli, S.; Pathak, S.; Mazzatenta, A.; Lieber, C. M.; Prato, M.; Bellamkonda, R. V.; Silva, G. A.; Kam, N. W. S.; Patolsky, F.; Ballerini, L. *Adv. Mater.* **2009**, *21*, 3970−4004.
(43) Baek, N. S.; Lee, J.-H.; Kim, Y. H.; Lee, B. J.; Kim, G. H.; Kim, I.-H.; Chung, M.-A.; Jung, S.-D. *Langmuir* **2011**, *27*, 2717−2722.
(44) Jing, G.; Wang, Y.; Zhou, T.; Perry, S. F.; Grimes, M. T.; Tatic-Lucic, S. *Acta Biomater.* **2011**, *7*, 1094−1103.
(45) Rosso, M.; Giesbers, M.; Schroën, K.; Zuilhof, H. *Langmuir* **2010**, *26*, 866−872.